Proceedings of the Canadian Society for Mechanical Engineering International Congress 2022
CSME Congress 2022
June 5-8, 2022, Edmonton, AB, Canada

INTEGRATION OF ARTIFICIAL NEURAL NETWORK AND FINITE ELEMENT METHOD FOR PREDICTION OF ELASTIC-PLASTIC DEFORMATION BEHAVIOUR NEAR CRACK TIPS

S.N.S. Mortazavi, A. Ince*
Department of Mechanical, Industrial and Aerospace Engineering, Concordia University, Montreal, Canada
*ayhan.ince@concordia.ca

Abstract—It has been widely accepted that stress and strain fields near the crack tip govern crack propagation behavior. In most cases, an elasto-plastic analysis is required to determine local stress and strain fields around the crack tip due to the high stress concentration. However, complexities of such analysis lead researchers to either employ modified elastic analyses to approximately address stress/strain fields near the crack tip, or consider cracks as micro notches and use the Neuber rule as an approximation method to estimate elasto-plastic stress/strain fields from elastic stress/strain fields in the vicinity of micro notch tips. Unfortunately, both approaches have limitations to provide generalized solutions. The present work aims to develop robust artificial neural network (ANN) models to obtain elasto-plastic stress, strain, and displacement fields near the crack tips by means of a numerical elastic solution rather than a complex elasto-plastic solution. In order to do so, two separate finite element models (FEMs) are implemented to analyze a cracked specimen, made of stainless steel (SS304), under mode (I) of loading in both elastic and elasto-plastic states. ANN models are developed to learn the relationship between elastic and elasto-plastic behavior of the material in the presence of cracks. The elastic and elasto-plastic FEMs are employed to generate the input and output numerical data, respectively, to train and validate the constructed ANN models. The results show that well-trained ANN models can efficiently and accurately predict the elasto-plastic stress, strain, and displacement fields around the crack tips on the basis of numerical elastic finite element solution under monotonic loading conditions.

Keywords-finite element analysis; artificial neural network; stress, strain, and displacement prediction

I. INTRODUCTION

In most cases, local stresses in the close proximity of the crack tip exceeds the material yield strength due to the high stress concentration at the crack tip. Subsequently, an elasto-plastic analysis is needed to determine local stress and strain fields at/near the crack tip. Unfortunately, such analysis methods are undesired due to the complexity, high computation time and large data in practical engineering applications. As a result, researchers tend to employ approximate linear elastic solutions to address the crack propagation response of materials in the presence of cracks. Two of the most famous models to determine stress and strain fields near the crack tip under elastic state are the Westergaard method [1] and Creager-Paris solution [2]. Both methods use the stress intensity factor (SIF) to characterize the elastic stress field near the tip of cracks and deep notches. Since the local stress/strain field around the crack tip governs the fatigue crack growth (FCG) behavior, the SIF range was introduced by Paris and Erdogan as a crack growth driving force to calculate the FCG rate based on linear elastic fracture mechanics (LEFM) [3]. Almost all approximate elastic models to deal with crack behavior of materials can be categorized into two main groups. First is the one that employs the SIF range itself as a driving force. Such an approach simply ignores the plastic deformation zone (PDZ) at the tip of the crack and/or the sharp notch. The second group uses the modified driving forces based on the SIF range to adjust them to account for small-scale plasticity. Most of such modifications are based on either the crack closure concept originally suggested by Elber and Newman [4] or based on the 'Unified Approach", employing both the maximum SIF and SIF range to quantify FCG rate [5]. One of the most recent and promising models in the latter category is the UniGrow model. The success of the UniGrow model is attributed to the fact that the model not only using the two-parameter driving force (i.e. both the maximum SIF and SIF range are accounted for in the formulation of the two-parameter driving force) but also utilizing the Neuber rule to transform the hypothetical elastic stress/strain fields, obtained by the LEFM approach, to actual elasto-plastic ones [5]. Unfortunately, even crack-closure and two-parameter driving force based models cannot account for relatively large-scale plasticity e.g. the short crack regime in which the PDZ size is comparable with crack length [6-8]. In addition, the application of the Neuber rule is limited to the blunt, deep and micro notches [9-11]. In other words, the succesful application of the Neuber rule to estimate actual elasto-plastic stress/strain fields from the hypothetical elastic stress/strain field in case of real crack geometries has not been carried out yet. It should be mentioned that it has been suggested that SIF-based driving force can be replaced by other

driving force parameters such as J-integral-based or crack tip opening displacement (CTOD) to account for large-scale plasticity [12]. However, calculating such driving forces requires computationally inefficient and complicated elasto-plastic finite element (FE) analyses. As a result, such approaches are often considered to be impractical for engineering applications [13]. That is why many researchers persist in applying LEFM models to quantify FCG rate, even in the case of large-scale plasticity.

Artificial neural networks (ANNs), as one of the most powerful machine learning algorithms have recently received much interest to characterize material deformation [14] and FCG behavior [15]. In the case of crack growth behavior, experimental FCG datasets have been utilized for training ANN to predict crack growth behavior [16]. A great potential has been observed for the prediction of FCG rates by such algorithms [17]. Training datasets must be sufficiently large and well-structured in order to obtain well-trained ANN models to provide accurate predictions. Unfortunately, experimental FCG data are generally limited. As a result, the application of such models has been limited to particular conditions, in which there are sufficient and well-structured data in hand [18]. In the present paper, new ANN models are developed to establish the relationship between elastic and elasto-plastic responses of a cracked plate body. Two independent FEMs are developed to obtain the stress, strain, and displacement datasets near the crack tip under elastic and elasto-plastic states for a plate made of grade 304 (SS304) stainless steel. The stress, strain, and displacement fields under the elastic state are used as the input data, and those datasets under the elasto-plastic state are set as the output data for ANN models. The results showed that the robust algorithms of ANN can establish the complex non-linear relationship(s) between well-organized input and output data. As a result, the well-trained ANN models are capable of offering accurate and efficient computational predictive methods to predict the elasto-plastic stress, strain, and displacement distribution around the crack tip through a linear elastic solution under monotonic loading. It should be mentioned that the presented modeling approach is not limited to notches or any other specific geometry or any loading conditions.

II. Modeling Methodology

ANN algorithms are able to extract complex patterns from a given dataset and determine interplay relationships among input and output variables. Dataset is referred to the sequence of numerical numbers as input(s) and corresponding output(s). The modeling framework of an ANN schematically shown in Fig. 1, presents one input layer, three hidden layers, and one output layer to represent the ANN model structure. The first step of training the ANN model is based on data preparation, such as data normalization. Data normalization puts all of the input data in the same range in the case of multivariable problems so that, the order of the magnitude for data cannot yield any influence on the training process. As shown in Fig.1, each layer includes different numbers of neurons. In the first layer, each neuron embeds one input variable. The value of each neuron is multiplied by a positive value called weight (W_{ij}) and results in an activated neuron (X_iW_{ij}). The higher weight makes a particular neuron have more impact on the output. The sum of all activated neurons may be added with a positive value called bias (b) and then is delivered to the next layer. The hidden layers embed an activation function in each neuron. Each neuron in a hidden layer receives the value from the previous layer as the input of its activation function. Then the output of the activation function is activated and transferred to the next layer. As the last step, the value generated by the last hidden layer is transferred to the output layer. The output layer presented in Fig.1 consists of only one neuron. It should be pointed out that the output layer in different problems may consist of multiple output variables. All the hyperparameters, such as weights, biases, the number of hidden layers, the number of neurons in each layer, and activation functions, are required to be appropriately determined to build a well-trained network model. A well-trained network should work for any new data, not introduced in training and validation stages. ANN developed by Keras [19] with Tensorflow as a high-level neural network application programming interface (API) is adopted in the present study to develop and train the network models. Generally, three groups of data are used in the development of ANN models. First, data classified as the training data and its usage briefly is discussed above. Second, data defined as the validation data used to validate the trained model(s) and chosen hyperparameters e.g. weights and biases. As mentioned before, all the hyperparameters are assigned to account for particular training datasets. Then the ANN model should be tested by another group of datasets known as validation data to confirm the model prediction capability while adjusting the hyperparameters . This process is repeatedly conducted until the ANN model with its updated weights and biases can account for not only training data but also for validation data as well. After completing the training and validation processes, the ANN model may be tested for new datasets which have not been used as either training or validation data to assess prediction performance of the model. The latter group of datasets is known as testing data. In the present study, the displacement and stress/strain distributions resulting from an elastic FE analysis are fed to the network as the inputs. Subsequently, displacement and stress/strain distributions resulting from an elasto-plastic FEM are assigned as the network outputs. It has been shown that with this modeling approach, ANN can determine the relationships among the elastic and elasto-plastic responses of the material in a cracked specimen body. In the present study, both the elastic and elasto-plastic FEMs were developed using the commercial FE software package, Abaqus to obtain the input and output datasets for the network models.

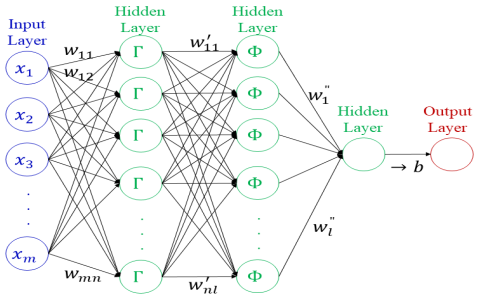

Figure 1. The schematic structure of ANN

The geometry and loading condition and all required geometric and material parameters to develop the FEMs are presented in Fig. 2, and TABLE I. Fig. 3 illustrates the area chosen around the crack tip to extract data from the FEMs. This area consists of 480 (40×12) elements and 1920 (480×4) Gauss points (GPs). As a result, the chosen area shown in Fig. 3 provides 1920 datasets for each crack length. Since the model is developed under plane strain conditions, four stress components and three non-zero strain components are obtained on each GP, and two displacement components are determined on each node. Stress and strain components at each GP are considered as datasets to train the ANN models for prediction of stress and strain distribution. Subsequently, the displacement components on each node are considered as specific datasets in the case of training the ANN model to predict the displacement field. Fig. 4 presents the matrices assigned as the input and output of the ANN model to predict the stress field around the crack tip. It should be emphasized that each matrix in Fig. 4 schematically has 1920 datasets generated by the FEM for one particular crack length.

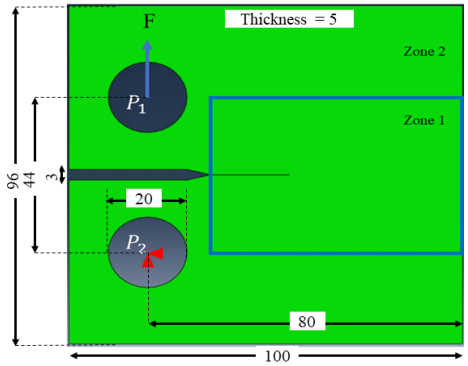

Figure 2. Description of FEM model, dimensions are in mm

TABLE I. DETAILED PARAMETERS FOR THE FEM

Material	SS304	**Elasto-plastic Model**	Bilinear isotropic hardening
Modulus of Elasticity (MPa)	195100	**Hardening Properties (MPa)**	570
Poisson's Ratio	0.267	**Mesh Size (mm)**	0.1 (in zone 1) 2 (in zone 2)
Yield Stress (MPa)	206	**Force (KN)**	20

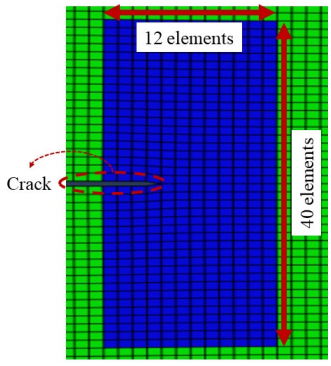

Figure 3. The area chosen around the crack tip to extract data from

However, ten different crack sizes are used to generate sufficient datasets to train promising networks. That being said, the number of datasets used in the present paper is 19200 (1920×10). The different crack lengths to provide the training, validation, and test data, discussed before are given in TABLE II. The input and output data matrices to train the ANN models to predict strain and displacement fields are similar to the data structure presented in Fig. 4. However, the number of components in each dataset is three and two in the case of strain field and displacement field, respectively, as mentioned earlier. In the present study, three different ANN models are trained, validated and tested to predict stress, strain, and displacement fields, separately. The number of neurons in the input layer is the number of input data (19200). And the number of neurons in the output layer is the number of outputs. The other characteristics of ANN models in terms of layers and neurons size are the same for all three models and are described in TABLE III.

III. RESULTS AND DISCUSSION

This section presents stress, strain, and displacement fields predicted by three different ANN models on the basis of the test data. The results of ANN models have been compared with the results obtained from elasto-plastic FEMs to assess the accuracy of proposed ANN models. It should be emphasized that the results of ANN models shown in this section correspond to test data i.e. new crack lengths, which have not been used during the training and validation of models. The crack tip in all of the contours presented in this section is at the origin of the coordinate system (x=0 and y=0). The key point that should be reminded here is that only the corresponding elastic fields are required by ANN models. to predict the elasto-plastic stress, strain, and displacement fields around the crack tip

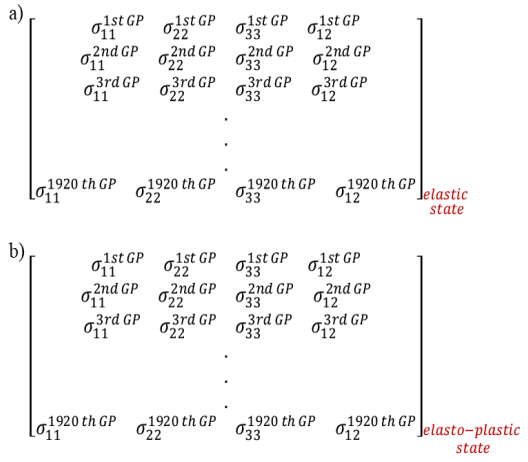

Figure 4. Schematic of training data for the presented ANN model to predict stress field around the crack tip. a) input data, b) output data

TABLE II. CRACK LENGTHS USED IN FEM TO GENERATE DATA

Data Type	**Crack Length (mm)**
Training data	1, 2, 3, 4, 5, 6, 7, 8, 9, 10
Verification data	1.5, 4.5, 7.5
Test data	2.5, 5.5, 8.5

TABLE III. STRUCTURE OF PRESENTED ANN MODELS

Number of Hidden Layers	Number of Neurons in the First Hidden Layer	Number of Neurons in the Second Hidden Layer
2	1024	512

In other words, the well-trained ANN models receive the hypothetical elastic stress, strain, and displacement fields as the input, and predict the corresponding actual elasto-plastic fields within 2 to 3 seconds. Fig. 5 a) and b) presents the results of the σ_{11} obtained by the trained ANN model and the elasto-plastic FEM for the crack length of 8.5 mm as one of the testing data. As shown in Fig. 5 a) and b), the distribution of σ_{11} around the crack tip predicted by the ANN model is very close to ones obtained by the elasto-plastic FEM. Fig. 5 c) also presents the percentage of error (POE) calculated using (1) between the values predicted by the ANN model and obtained by FEM. As shown, the POE is between -8 to +6 percent in this case. The number of GPs with relatively higher error (such as -8 or +6 percent) is significantly smaller than those with lower POE.

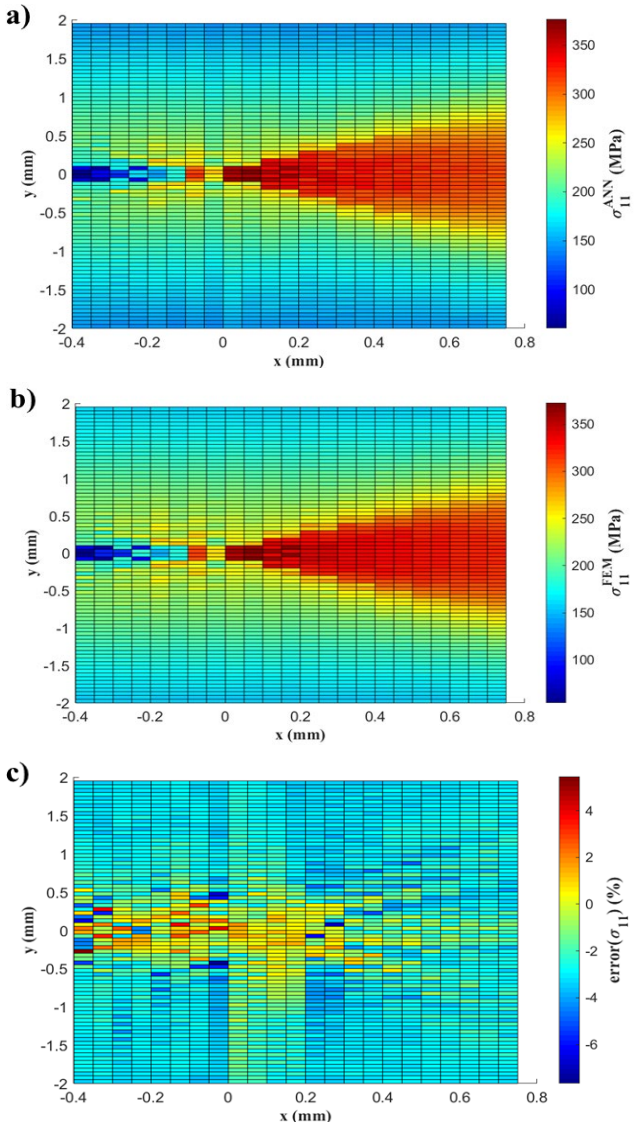

Figure 5. σ_{11} distribution of crack size of 8.5 mm. a) ANN prediction, b) FEM results, c) POE

Fig. 6 shows the results of the ANN model and FEM for σ_{22} as the second component of stress tensor around the crack tip for the crack length of 8.5 mm. As shown, the distribution of σ_{22} has been predicted accurately around the crack tip. The POE obtained by (1) is shown in Fig. 6. The POE for the second component of the stress tensor, σ_{22} is in the range of -8 and +6 percent in this case. Figs. 5-6 show the accuracy of two stress components (σ_{11} and σ_{22}) as examples of the stress field around the crack tip for the crack length of 8.5 mm. The results showed that the POE for the other two components (σ_{33} and σ_{12}) is less than 10%. The elasto-plastic stress fields predicted by the ANN model have been compared with the ones obtained by FEM for the crack lengths of 2.5 and 5.5 mm as the other test data described in TABLE II as well. The maximum POE in those cases is less than 10%.

$$POE = \frac{\sigma^{ANN} - \sigma^{FEM}}{\sigma^{FEM}} \times 100 \,. \quad (1)$$

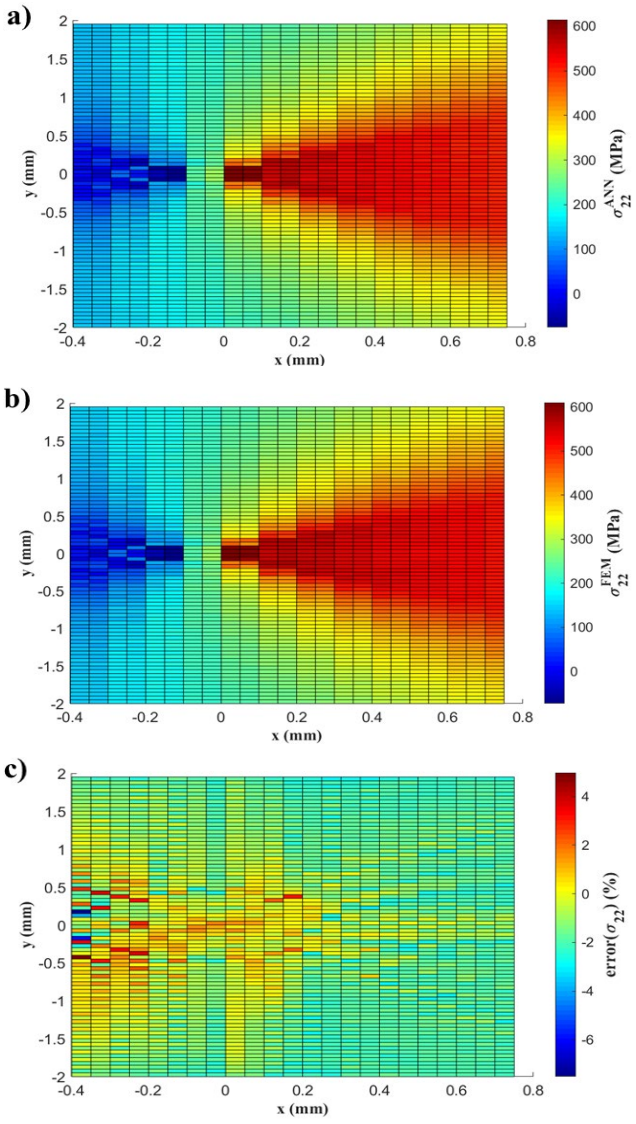

Figure 6. σ_{22} distribution of crack size of 8.5 mm. a) ANN prediction, b) FEM results, c) POE

Fig. 7 a) and b) shows the results of ε_{11} as the first strain tensor component predicted by the ANN model and elasto-plastic FEM for the crack length of 5.5 mm. As shown in Fig. 7, the POE calculated using (1) is between -20 and +5 percent for this case.The contour of error in Fig. 7 c) shows that the values of only two GPs behind the crack tip are close to -20%. It means the POE would be between -10 and +5 percent by ignoring those two GPs. Fig. 8 presents the results of the second component of the strain tensor, ε_{22}, predicted by the ANN model and elasto-plastic FEM for the crack size of 5.5 mm. For this case, the POE is in the range of -4 to +14 percent. Similar to the previous case, the values of POE only for two GPs is around 14%. It means the POE is approximately between -4 to +8 percent for most GPs. Fig. 7-8 show the results of two strain components (ε_{11} and ε_{22}) as the examples of strain components for the crack size of 5.5 mm. The results showed that the maximum of POE in the case of ε_{12} as the third strain tensor component is less than 20% for the crack size of 5.5 mm. The results showed that the POE for predicted strain components for 8.5 and 2.5 mm crack sizes is less than 20%.

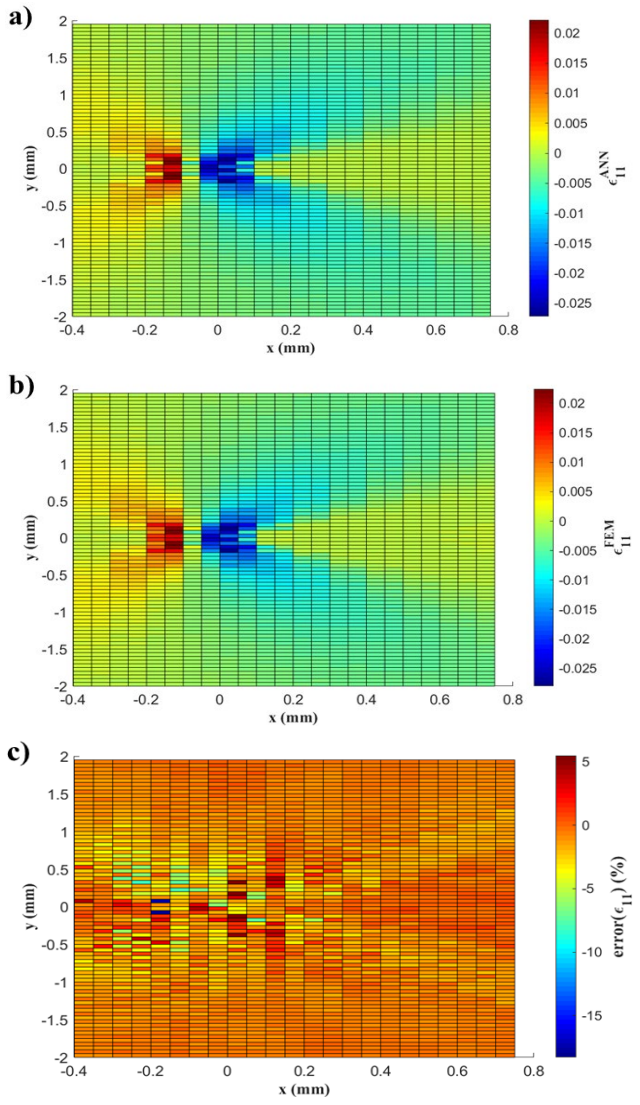

Figure 7. ε_{11} distribution of crack size of 5.5 mm. a) ANN prediction, b) FEM results, c) POE

Fig. 9 a) and b) presents the results of u_2 as the second component of the displacement vector predicted by the ANN model and elasto-plastic FEM for the crack length of 2.5 mm. The distribution of the predicted u_2 agress well with the one predicted by elasto-plastic FEM. The POE is between -30 to +5 percent in this case. As discussed before, the displacement values as datasets for training the ANN model have been extracted from the nodes in the FEMs. However, the stress and strain datasets have been extracted from the GPs. Each element has four GPs in the presented FEM. On the other hand, each node is commonly shared between four elements. As a result, the number of displacement datasets is significantly smaller than stress and strain datasets. Therefore it is considered that the accuracy of displacement prediction is less than that in the case of stress and strain predictions due to smaller data size. Fortunately, the accuracy in all cases discussed so far can be improved by increasing the number of training data discussed in TABLE II. The results showed that the maximum POE for the u_1 in the case of crack length of 2.5 mm, and for u_1 and u_2 for the crack sizes of 5.5 and 8.5 as the other test data is less than 30%.

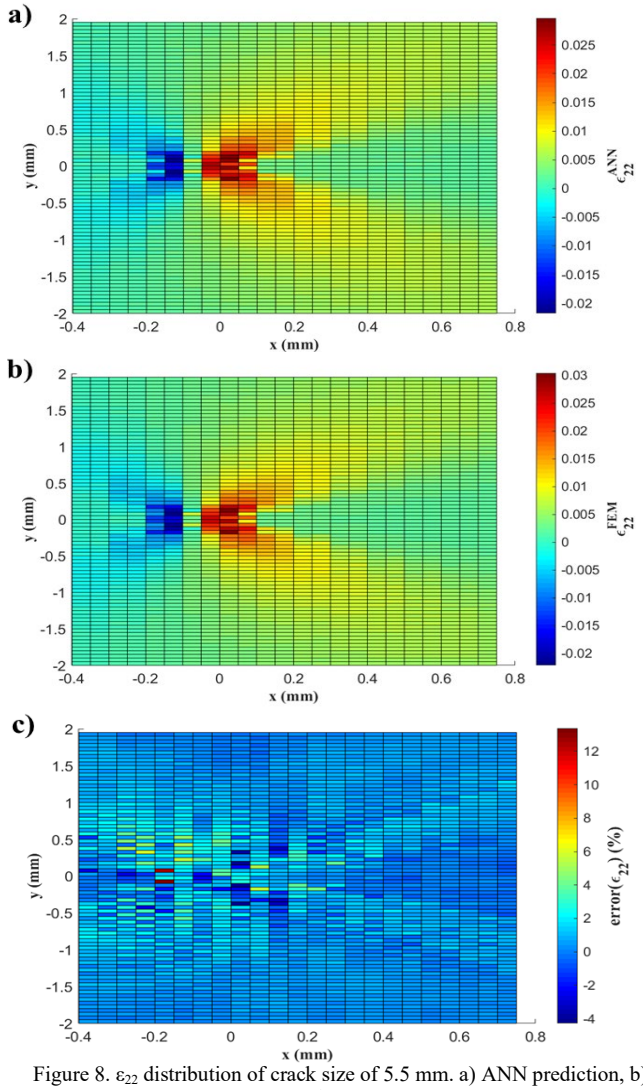

Figure 8. ε_{22} distribution of crack size of 5.5 mm. a) ANN prediction, b) FEM results, c) POE

IV. CONCLUSION

In the present study, artificial neural network (ANN) models are developed as predictive models to determine the relationship(s) between elastic and elasto-plastic responses of stainless steel (SS304) in a cracked specimen around the crack tip. The stress, strain, and displacement fields obtained by the elastic finite element model (FEM) have been used as the input data to the ANN models. Subsequently, the ones obtained by the elasto-plastic FEM have been employed as the output data to train ANN models. The results showed that the well-trained ANN models with the proposed modeling approach can accurately and efficiently predict the elasto-plastic stress, strain, and displacement fields near the crack tip by only using the corresponding elastic fields. Such predictive modeling capability to compute elastic-plastic stress, strain and displacement fields near cracks provides a great advantage over complex elastic-plastic FE analyses due to its computational efficiency, and low cost.

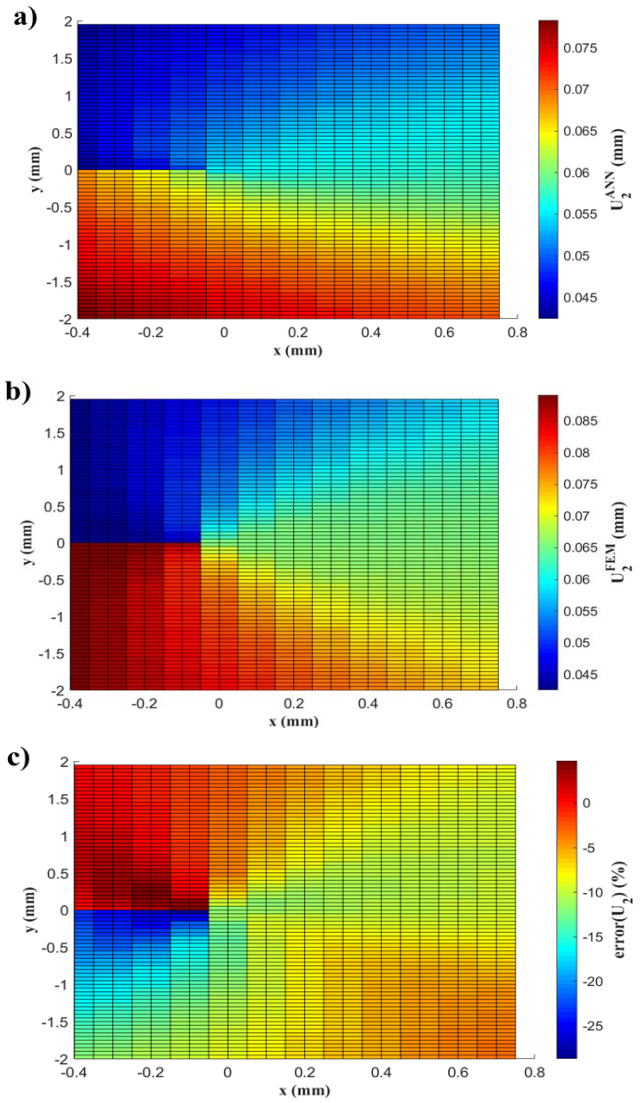

Figure 9. u_2 distribution of crack size of 2.5 mm. a) ANN prediction, b) FEM results, c) POE

ACKNOWLEDGMENT

The authors would like to acknowledge the financial support of Natural Sciences and Engineering Research Council of Canada (NSERC) (DGECR-2018-00232).

REFERENCES

[1] G. C. Sih, "On the westergaard method of crack analysis", Int J. Fracture, vol. 2, pp. 628-631, 1966.

[2] M. Creager, P. C. Paris, "Elastic field equations for blunt cracks with reference to the stress corrosion cracking", Int. J. Fracture, vo;. 3, 247, 1967.

[3] P. Paris, F. Erdogan, "A critical analysis of crack propagation laws", J. Basic Eng., vol. 85, pp. 528-533, 1963.

[4] J. Newman, "Prediction of fatigue crack growth under variable-amplitude and spectrum loading using a closure model", Design of fatigue and fracture resistant structures, ASTM International, pp. 255-277, 1982.

[5] A.H. Noroozi, G. Glinka, S. Lambert, "A two parameter driving force for fatigue crack growth analysis", Int. J. Fatigue, vol. 27, pp. 1277-1296, 2005.

[6] D. Bang, A. Ince, L. Tang, "A modification of UniGrow 2-parameter driving force model for short fatigue crack growth", Fatigue Fract. Eng. Mater. Struct., vol. 42, pp. 45-60, 2019.

[7] D. J. Bang, A. Ince, M. Noban, "Modeling approach for a unified crack growth model in short and long fatigue crack regimes" Int J Fatigue, vol.128, pp.105182, 2019.

[8] D. J. Bang, A. Ince, "A short and long crack growth model based on 2-parameter driving force and crack growth thresholds", Int J Fatigue, vol.141, pp.105870, 2020.

[9] A. Ince, G. Glinka and A. Buczynski, "A Computational Modeling Technique of Elasto-Plastic Stress-Strain Response for Notched Components", International Journal of Fatigue, vol. 62, pp.42-52, 2014.

[10] A. Ince, "Numerical Validation of Elasto-plastic Stress and Strain Analysis Model for Notched Components Subject to Non-Proportional Loadings", Theoretical and Applied Fracture Mechanics, vol. 84, pp.26-37, 2015

[11] A. Ince, D. Bang, "Deviatoric Neuber method for stress and strain analysis at notches under multiaxial loadings", Int. J. Fatigue, vol. 102, pp. 229-240, 2017.

[12] J. Hou, K. Tang, H. Wu, "Short review on multiscale short fatigue crack growth model", Mater. Des. Process Commun., vol. 2, e93, 2020.

[13] J. Wang, W. Jiang, Y. Li, Q. Wang, Q. Xu, "Numerical assessment of cyclic J-integral for predicting fatigue crack growth rate", Eng. Frac. Mechanics, vol. 205, pp. 455-469, 2019.

[14] F. Hajializadeh, and A. Ince, "Integration of artificial neural network with finite element analysis for residual stress prediction of direct metal deposition process", Materials Today Communications vol. 27, pp.102197, 2021.

[15] J. Chen, Y. Liu, "Fatigue modeling using neural networks: A comprehensive review", Fatigue Fract. Eng. Mater. Struct., 2021.

[16] S. Mortazavi, A. Ince, "An artificial neural network modeling approach for short and long fatigue crack propagation", Computational Materials Science, vol. 185, pp. 109962, 2020.

[17] S. Mortazavi, A. Ince, "A radial basis function artificial neural network methodology for short and long fatigue crack propagation", Proc. Can. Soc. Mech. Eng. Int. Congr 2021, 2021.

[18] S. Himmiche, S. Mortazavi, A. Ince, "Comparitive study of neural network-based models for fatigue crack growth predictions of short cracks", J. Peridyn. Nonlocal Model, 2021.

[19] N. Kektar, E. Santana, Deep Learning with Python, Springer, 2017.